Available online at www.sciencedirect.com
ScienceDirect
Catalysis Today 118 (2006) 307–314
CATALYSIS TODAY
www.elsevier.com/locate/cattod

Limonene oxidation over V_2O_5/TiO_2 catalysts

P. Oliveira [a], M.L. Rojas-Cervantes [b], A.M. Ramos [a], I.M. Fonseca [a], A.M. Botelho do Rego [c], J. Vital [a,*]

[a] *REQUIMTE, Departamento de Química, FCT-UNL, 2829-516 Caparica, Portugal*
[b] *Departamento de Quimica Inorgánica y Quimica Tecnica (U.N.E.D.), Paseo Senda del Rey n° 9, 28040 Madrid, Spain*
[c] *CQFM-CI, IST, Av. Rovisco Pais, 1049-001 Lisboa, Portugal*

Available online 22 August 2006

Abstract

Vanadia-titania catalysts prepared by different sol–gel procedures were studied as heterogeneous catalysts for the liquid phase oxidation of limonene. The catalysts were characterized by XRD, XPS, ICP and nitrogen adsorption. According to the XRD results the catalyst samples can be divided in two different groups: anatase samples and anatase + rutile samples. XRD signals of vanadia are not found in the diffractograms.

The main reaction products are polymers. Limonene oxide, limonene glycol, carveol and carvone are obtained in small amounts. A number of autoxidation products, alcohols, aldehydes and ketones, are also obtained.

The effects of titania composition on the reaction orientation are discussed.

Keywords: Limonene oxidation; Vanadia-titania; Anatase; Rutile

1. Introduction

Limonene is the main component of citrus oil and it can be easily obtained from citrus peal, which is a waste material of the fruit juice industry. Limonene epoxide is a key raw material for a wide variety of products such as pharmaceuticals, perfumes and food additives. It is usually epoxidized *via* the stoichiometric peracid route, however, due to environmental reasons this process is becoming increasingly unacceptable. The limonene liquid phase oxidation may proceed by two distinct pathways: (a) epoxidation, leading to limonene-1,2-epoxide (limonene oxide) as the main product, or (b) allylic oxidation and autoxidation, carveol and carvone being obtained mainly, although a large number of other products is also formed (since the reaction proceeds through a free radical chain reaction mechanism). In acidic reaction media, the limonene oxide may be hydrolysed forming limonene glycol [1–3] (Scheme 1).

Supported vanadium oxide catalysts are active in a wide range of applications, such as selective oxidations of several alkanes and alkenes, reduction of nitrogen oxides to ammonia, etc. [4]. Supported vanadium oxide catalysts can be prepared by several methods, such as impregnation, co-precipitation, liquid-phase grafting and chemical vapour deposition [5]. The preparation method does not seem to have influence in the vanadium oxide configuration obtained after calcination treatments. However, it seems to strongly affect its dispersion on the support surface [4]. It was shown, by different characterization methods [6–8] that the vanadium phase may be present on the surface of the oxide support as a crystalline V_2O_5, as well as a two-dimensional vanadium overlayer, for values of vanadium loadings higher than the monolayer coverage. Although it is established that a support should be inert, it is known that the activity of the vanadium oxide is greatly affected by the properties of the support oxide used [4].

TiO_2 is a suitable support, although there is some controversy in the literature concerning to the role of the support crystalline phase (anatase and rutile) on the catalytic characteristics of the V_2O_5/TiO_2 catalysts. The phase transition from anatase into rutile is known to occur at temperatures about 823 K [7], in the presence of vanadium. This transition is accompanied by the incorporation of V^{4+} into the rutile structure. Generally, it is stated that anatase is a more active support than rutile [9]. This may be due to the fact that the properties of the vanadium species present on the surface of the rutile

* Corresponding author. Tel.: +351 212948385; fax: +351 212948385.
E-mail address: jmv@dq.fct.unl.pt (J. Vital).

0920-5861/$ – see front matter
doi:10.1016/j.cattod.2006.07.032

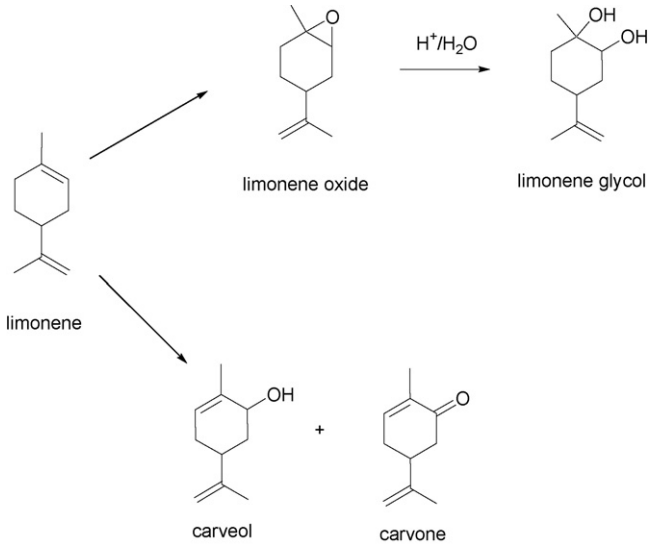

Scheme 1.

polymorph phase resemble the properties of those of pure V_2O_5, while those present on the surface of the anatase phase have different acid-basic and redox properties [7]. The activity of the V_2O_5/TiO_2 is often related with the solid acidity. Both Lewis and Brönsted acid sites may be present as it was determined by IR of adsorbed pyridine [10].

This work reports the oxidation of limonene in the liquid phase, over V_2O_5/TiO_2, using *tert*-butyl hydroperoxide (*t*-BHP) as oxygen donor. The catalysts were prepared by different sol–gel techniques.

2. Experimental

2.1. Materials and solvents

The vanadyl acetylacetonate (95 wt.% purity) was supplied by Aldrich. The ethylene glycol was from Riedel-de-Haën and nitric acid was from Panreac. All the other reactants used in the synthesis of the V_2O_5/TiO_2 catalyst samples were supplied by Fluka. Acetone, *t*-butanol and *t*-butylhydroperoxide (70 wt.%) were purchased from Aldrich. Limonene (98%) was supplied by Fluka.

2.2. Catalyst preparation

Six V_2O_5/TiO_2 samples were prepared by different methods. In all cases the theoretical vanadium content was kept constant (5 wt.%). For all the catalyst samples prepared the following molar ratios were used: water/titanium isopropoxide, 5; alcohol/titanium isopropoxide, 15; HNO_3/titanium isopropoxide, 0.2. Finally, all the dried gels were calcined to obtain the V_2O_5/TiO_2 samples with the following program: heating from room temperature up to 100 °C, holding 30 min, then heating up to 300 °C and holding 60 min, and finally heating up to 500 °C and holding for 180 min. For all the samples, the heating rate used was 3 °C min^{-1}.

The preparation details of the individual catalyst samples are given below.

2.2.1. Sample 1

An aqueous solution of nitric acid was added dropwise to a flask containing a propanolic solution of titanium(IV) isopropoxide (TIP) and vanadyl acetylacetonate (VOAA) in the appropriate amounts under continuous stirring. At the gelling point, the stirring was stopped and the gel was aged at room temperature for 3 days. The final gel was dried in a vacuum oven at 80 °C for 14 h.

2.2.2. Sample 2

The precursor gel of titanium oxide was prepared as for synthesis 1, but without adding VOAA. Once the gel was aged and dried, this was impregnated in a rotavapor with a propanolic solution of VOAA at 70 °C.

2.2.3. Sample 3

This V_2O_5/TiO_2 sample was synthesised by the modified sol–gel method with the procedure developed by Dosch et al. [11], although in our case the sodium hydroxide was replaced by an organic base. This method is referred to as a modified sol–gel method because it differs from the traditional sol–gel procedure in that a soluble intermediate is formed in a non-aqueous medium prior to hydrolysis. VOAA was dissolved in a solution of tetramethylammonium hydroxide (10 wt.%) in methanol. Then, TIP was slowly added to the hydroxide solution to obtain a clear soluble intermediate. This intermediate was rapidly added to a 1:10 by volume solution of water and acetone. The slurry was continuously stirred until the particles were suspended in the solution. Finally, the precipitate was collected by filtering and dried in an oven at 80 °C for 14 h.

2.2.4. Sample 4

TIP was slowly added to a solution of tetramethylammonium hydroxide (10 wt.%) in methanol and stirred until a very thick soluble intermediate was formed. This intermediate was rapidly added to a 1:10 water:acetone solution. The resulting slurry was stirred until homogenisation, then filtered, rinsed with acetone and dried in an oven at 80 °C for 14 h. Afterwards, the vanadium active metal was incorporated via ion exchange. Before loading the metal, the hydrous titanium oxide was changed to its protonic form by treatment with 0.1 M sulphuric acid at pH 3 for 2 h. Then, it was treated with a 0.1 M solution of VOAA in propanol, stirred for 3 h, filtered and dried in an oven at 80 °C for 14 h.

2.2.5. Sample 5

This sample was prepared [12] by refluxing VOAA in 2-metoxiethanol at 120 °C for 90 min. After cooling until 90 °C, TIP was added and the solution was again refluxed at 120 °C for 120 min, until a clear solution was obtained. Then the aqueous solution of nitric acid was added dropwise. The gel thus formed was aged for 3 days at room temperature and dried in a vacuum oven at 80 °C for 14 h.

2.2.6. Sample 6

This sample was prepared by using an ethylene glycol solution as complexing agent of the metal atom [13]. The VOAA was refluxed in ethylene glycol at 80 °C for 150 min. The amount

of ethylene glycol was 100 times higher than the stoichiometric one for the formation of the vanadium complex. Then, once cooled and added TIP, the solution was again refluxed at 80 °C for 45 min. After cooling at room temperature, the aqueous nitric acid solution was added dropwise under continuous stirring. The gel formed was aged at room temperature for 3 days and dried in an oven at 80 °C for 14 h.

2.2.7. Sample TiO_2

In order to check the catalytic activity of the titania support of sample S6, a TiO_2 support sample was prepared in a similar way to S6, but without adding VOAA.

2.3. Catalyst characterization

The diffraction patterns were measured with a Philips 1730/10 diffractometer, using Cu Kα radiation. The textural characterization of the V_2O_5/TiO_2 materials was obtained from physical adsorption of nitrogen at 77 K in a Micrometrics ASAP 2010 V1.01 B instrument. An amount of ca. 0.4 g of sample was outgassed at 150 °C for 16 h, until getting a residual vacuum of 5×10^{-3} mmHg. The surface area was calculated using the BET equation. Micropore volume (V_{mic}) and the average micropore diameter (d_{mic}), was calculated using the Horvath-Kawazoe method; the mesopore volume (V_{mes}) and the average mesopore diameter (d_{mes}), were obtained by applying the BJH pore analysis to the desorption isotherm.

Inductively coupled plasma atomic emission spectroscopy (ICP) was performed in a Jobin-Yvon (Ultima) instrument.

X-ray photoelectron spectroscopy (XPS) was carried out on a XSAM800 (KRATOS, Manchester, UK) X-ray spectrometer operated in the fixed analyzer transmission (FAT) mode with a pass energy of 20 eV, using a non-monochromatic radiation from Mg anode (main $h\nu = 1253.6$ eV). The pressure in the analysis chamber was in the range of 1×10^{-9} Torr; power was 130 W. With this low power, vanadium reduction is avoided [14]. Anyway, the vanadium region was acquired in first place. To account for the sample surface charging, the binding energy scale in the XPS spectra was aligned taking as reference the Ti $2p_{3/2}$ core line at 458.5 eV [15,16]. For peak fitting, Gaussian and Lorentzian products were used after the subtraction of source satellites and a Shirley background.

2.4. Catalytic experiments

Two sets of experiments were performed in a batch reactor at 60 °C, under atmospheric pressure and magnetic stirring, using an excess of oxidant, i.e. *t*-butyl hydroperoxide (*t*-BHP) aqueous solution and a mixture of acetone and *t*-butanol as solvent (9:1 molar ratio). This solvent was chosen in order to ensure homogeneous liquid phase and simultaneously to avoid solvent oxidation. In the first set the reactions were carried out with concentrated *t*-BHP (70%, w/w). Typically, the reactor was loaded with 14.5 mmol of limonene and the oxygen donor, in a 1:8 molar ratio along with 50 mg of catalyst and 50 mL of solvent. In the second set, diluted *t*-BHP (3% in acetone) was used; all the other reaction conditions were kept constant.

Samples were taken periodically and analysed by GC and GC–MS on a 30 m × 0.25 mm DB-1 column, from J&W, using *n*-nonane as internal standard.

3. Results and discussion

3.1. Catalyst preparation

In the sol–gel process there are numerous synthesis parameters, which affect the reaction rates and the uniformity of the hydrolysis and polymerisation [17–19]. It has been demonstrated that the different reaction pathways followed when acidic, basic, or complexing agents are added, do exert a direct influence on the size, shape, and state of aggregation of the particles formed, thus modifying the crystallization and sintering behaviour of oxide materials derived from polycondensates [20]. One of these parameters is the water/alkoxide ratio used. Thus, Yoldas [20] found that titanium oxide obtained via hydrolytic polycondensation of undiluted $Ti(OC_2H_5)_4$ was formed only by the anatase phase, whereas that produced via highly diluted alkoxide consisted of a mix of anatase and rutile phases.

Another factor which affects the structural properties of the oxides obtained is the pH at which the synthesis was carried out. Thus, López et al. [21] found that in the titania formed from titanium isopropoxide (TIP) at pH 9, the main phase was anatase, and however, a small amount of rutile was detected also for the sample prepared at pH 3, in samples calcined at 600 °C. The stabilization of anatase phase by the surface hydroxyl groups has been also previously reported [22]. On the other hand, it has been found [23] that when the ethylene glycol is used as chemical additive, it forms some insoluble materials (for example, adducts or complexes) with the titanium alkoxides as soon as this is added into the diol (an homogenous solution is not obtained).

In the present work, several samples have been prepared by sol–gel method in different conditions. They have been synthesised at different pH values, derived from the use of tetramethylammonium hydroxide solution or nitric acid solution. In addition, the dilution of the alkoxide used (TIP) was different because, although the same amount of water was employed in all syntheses, in some cases (S3 and S4) acetone was also used as solvent. The sample S6 was prepared using ethylene glycol as a complexing agent and in this case no clear soluble intermediate was obtained, at difference of the samples prepared with tetramethylammonium hydroxide solution. Considering all the above exposed, the structural properties of the titanium oxides obtained are influenced by the synthesis conditions used, and different crystalline phases are obtained. At the same time, the activity of V_2O_5/TiO_2 catalysts is greatly affected by the properties of the support oxide used [4].

3.2. Catalyst characterization

3.2.1. X-ray diffraction

Powder XRD patterns of the vanadium containing samples supported on TiO_2 exhibit only the crystalline phases of the

Table 1
Molar fractions and average crystallite size of anatase and rutile for the calcined V_2O_5/TiO_2

Sample	Molar fraction		d (Å)	
	Anatase	Rutile	Anatase	Rutile
S1	1.0	0.0	237	–
S2	0.83	0.17	311	355
S3	0.91	0.09	190	180
S4	1.0	0.0	376	–
S5	1.0	0.0	288	–
S6	1.0	0.0	282	–

support. No vanadium compound is detected in the diffractograms, which means that either the vanadium phase is present as an amorphous phase or the microcrystalline size is less than 4.0 nm. For the samples S1, S4, S5 and S6, only anatase phase is detected. For the rest of the samples (S2 and S3) there is a mixture of anatase and rutile. The proportion of each one of the phases has been calculated by using the following equation [24]:

$$x_R = \frac{1}{1 + 1.26(I_A/I_R)},$$

where x_R is the molar fraction of rutile, I_A the intensity corresponding to the (1 0 1) diffraction peak of anatase, and I_R is the intensity corresponding to the (1 1 0) diffraction peak of rutile. The values of average crystallite size have been derived from the (1 0 1) diffraction peak for anatase and the (1 1 0) diffraction peak for rutile, by applying the Scherrer equation [25]. The results are collected on Table 1.

3.2.2. Textural characterization

Table 2 reports the BET surface areas, micropore and mesopore volumes, as well as micro and mesoporous diameters, of all the catalyst samples and of the support (TiO_2), calcined at 550 °C. Generally, the BET surface areas remained practically unchanged, except for the catalysts S3 and S6, which indicates that the introduction of the vanadium phase did not induce any remarkable decrease in the surface area of the supported catalysts when compared with the surface area of the TiO_2. For the catalyst S3, where V_2O_5 is supported on the two phase (anatase + rutile) support, the surface area slightly increased.

It is well known that crystallization is highly influenced by the hydrolysis conditions [26]. Thus, during the condensation process, the formation of the kinked chains of edge-sharing octahedra corresponding to anatase appears more probable than the formation of the straight chains typical of rutile. In fact, amorphous TiO_2 crystallizes into anatase below 400 °C, which is further converted to rutile from 600 to 1100 °C [27], the rates of transformation being markedly influenced by the particle size or the presence of impurities [28]. Although it has been reported that this behaviour appears to be associated with a concomitant decrease in specific surface area [7,29], we observed that the S_{BET} values for the samples containing anatase + rutile are higher than those containing only anatase. For the catalyst S6 the decrease in the surface area may be attributed to pore blockage.

Table 2
Textural characteristics of the calcined samples

Catalysts	V_{mic} ($cm^3\ g^{-1}$)	V_{mes} ($cm^3\ g^{-1}$)	d_{mic} (Å)	d_{mes} (Å)	S_{BET} ($m^2\ g^{-1}$)
S1	0.008	0.054	10.9	162.0	15.9
S2	0.008	0.036	10.6	123.3	17.0
S3	0.013	0.096	8.7	142.5	27.5
S4	0.005	0.028	11.9	147.4	11.4
S5	–[a]	0.071	–[a]	265.0	11.1
S6	–[a]	0.041	–[a]	168.5	9.9
TiO_2	0.006	0.042	17.3	93.9	17.5

[a] Not determined.

3.2.3. X-ray photoelectron spectroscopy

The ratio between the amount of vanadium determined by XPS and that determined by ICP (V_{XPS}/V_{ICP}) yields information about the homogeneity of the vanadium distribution [30]. For all the catalyst samples, but S6, V_{XPS}/V_{ICP} (Table 3) is higher than unity, which is an indication that the V_2O_5 is heterogeneously distributed, being preferentially located on the external surface of the support particles.

Sample S5 exhibits the highest vanadium loading and the highest heterogeneity in vanadium distribution. For the catalyst S6, the low value obtained for the ratio V_{XPS}/V_{ICP} suggests that the vanadium oxide is preferentially located deeply inside the porous system of the support particles, thus leading to the observed decrease in the BET surface area.

The XPS spectra in the regions O 1s, Ti $2p_{3/2}$ and V $2p_{3/2}$ were recorded for all the samples. All the catalyst samples spectra in the Ti $2p_{3/2}$ region (not shown) exhibit a maximum at about 458.5 eV, which corresponds to bulk TiO_2 [31]. Fig. 1 shows the XPS spectra of the regions O 1s and V $2p_{3/2}$ of samples S1, S4 and S6. The high-resolution spectra of the catalyst samples in the V $2p_{3/2}$ region show two peaks at about 516.8 ± 0.2 and 515.6 ± 0.2 eV, except for the catalyst sample S4, which can be attributed to vanadium species present in different oxidation states. These binding energies are characteristic of V^{5+} and V^{4+} valence forms, respectively [32]. For all the catalyst samples, except for the catalyst S6, the peak at about 516.8 eV is more intense than the peak characteristic of the V^{4+} species. For the sample S4 only the peak characteristic of V^{5+} is observed, and for the catalyst S6 both peaks show similar intensity. This observation, similar to those previously reported for V/ZrO_2 catalysts [33], suggests that the vanadium oxidation state increases with loading. The O 1s spectra obtained for all the catalyst samples exhibit two fitting peaks at about 530 ± 0.2 eV characteristic of the lattice oxygen of the

Table 3
Vanadium content as determined by XPS and ICP analysis

Sample	V_{ICP} (%)	V_{XPS} (%)	V_{XPS}/V_{ICP}
S1	4.52	9.01	2.00
S2	4.09	8.27	2.02
S3	4.61	8.27	1.79
S4	7.63	9.91	1.30
S5	4.28	12.61	2.94
S6	1.71	0.77	0.45

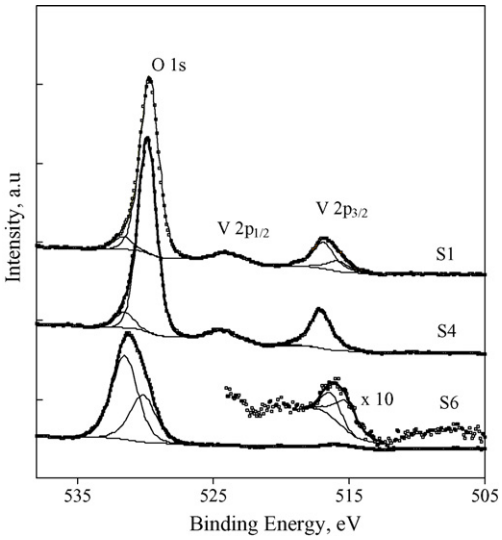

Fig. 1. XPS spectra of the V 2p and O 1s region for the catalyst samples S1, S4 and S6, including the peak fitting for the V $2p_{3/2}$ and O 1s spectra.

V_2O_5, and a less intense peak, with a maximum at about 531.6 ± 0.2 eV, which may be assigned to the oxygen atoms belonging to organic contamination present on the surface of the transition metal oxides.

3.3. Catalytic experiments

Limonene oxidation over the different V_2O_5/TiO_2 catalysts tested, using concentrated and diluted *t*-BHP as oxidant, yields polymers as main products. Limonene oxide, limonene glycol, carveol and carvone are formed in small amounts. Trace amounts of products, such as perillaldehyde, *p*-mentha-1(7),8-dien-2-ol, *p*-mentha-2,8-dien-1-ol as well as several unidentified substances are also formed. Although a complete identification of these last products has not been possible, the similarity between their mass spectra and that of carvone suggests that they are carbonyl compounds with the skeleton of *p*-menthene. All these

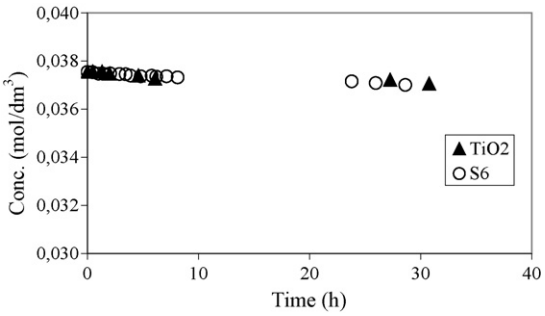

Fig. 2. Liquid phase limonene oxidation. Concentration profiles of limonene obtained for the experiments carried out over the catalyst S6 and the support TiO_2, using diluted *t*-BHP as oxygen donor.

terpenic alcohols, aldehydes and ketones, which are likely to be formed by limonene autoxidation, will be further in this text lumped under the designation of ''others''.

Table 4 shows initial turnover frequency (TOF), maximum conversion and selectivity values obtained for the experiments carried out with diluted *t*-butylhydroperoxide (series D) and with concentrated hydroperoxide (series C). Regarding TOF, the experiments carried out with the catalyst S6, exhibit extreme contradictory behaviour: in series D (diluted *t*-BHP) S6 exhibits the lowest TOF; in series C (concentrated *t*-BHP) S6 exhibits the highest TOF. These results suggest that, for the experiments carried out with diluted *t*-BHP, the oxidation reaction takes place exclusively on the vanadium sites. With sample S6, in which vanadium is preferentially located deeply inside the particles pore system, there is practically no reaction probably due to internal diffusion limitations. Since it is precisely with this catalyst sample that the highest TOF in series C is observed, we arrive to the conclusion that, under these reaction conditions, titanium is also active, probably in the hydroperoxide decomposition. Consequently a high number of free radicals are probably generated and limonene conversion is likely to proceed *via* autoxidation. The coincidence between the limonene kinetic curves obtained for the catalyst S6 and for the TiO_2 support (Fig. 2), confirms

Table 4
Liquid phase limonene oxidation carried out over V_2O_5/TiO_2 catalysts, using concentrated (C) and diluted (D) *t*-BHP as oxygen donor

Sample	Conversion[a]	Selectivity[b]				TOF[c]
		Limonene oxide	Limonene glycol	Carvone	Polymer	
S1_C	93.1	–	11.6 (40)	5.3 (91)	73.3 (93)	8.89
S2_C	97.8	2.6 (10)	1.6 (30)	5.2 (69)	83.8 (97)	7.79
S3_C	97.6	6.9 (12)	1.7 (80)	0.5 (25)	87.2 (97)	0.36
S4_C	96.8	–	12.9 (6)	5.1 (97)	78.7 (97)	2.76
S5_C	98.1	1.2 (1)	7.3 (1)	5.1 (80)	84.9 (98)	7.95
S6_C	95.1	–	9.1 (74)	2.3 (33)	81.8 (95)	10.30
S1_D	96.1	1.8 (4)	7.4 (4)	3.9 (4)	93.7 (96)	1.45
S2_D	95.4	6.5 (11)	41.5 (1)	7.4 (6)	81.2 (95)	0.82
S3_D	47.2	14.7 (6)	15.4 (2)	3.9 (23)	89.3 (47)	0.11
S4_D	96.7	8.1 (16)	2.7 (68)	4.3 (16)	78.7 (97)	1.58
S5_D	90.5	23.0 (16)	17.1 (33)	19.9 (16)	77.8 (91)	1.95
S6_D	6.3	51.2 (0.2)	15.5 (6)	–	–	3.6×10^{-7}

[a] Maximum conversion achieved.
[b] Maximum selectivity. The corresponding conversion level is shown between parenthesis.
[c] Initial turnover frequency.

that the catalytic activity observed for the catalyst S6 with diluted hydroperoxide is mainly due to the TiO_2 support.

As expected, the highest TOF values are obtained in series C, due to the severe reaction conditions. The highest selectivities for limonene oxide are obtained in series D, at higher limonene conversions (shown inside parenthesis). Similarly to the observations reported for the reaction carried out over carbon anchored cobalt acetylacetonate [34], limonene oxide is likely to be a primary reaction product, directly formed on the vanadium sites, being readily polymerised under the severe reaction conditions used in series C.

Fig. 3 shows the concentration profiles obtained for limonene, limonene oxide and polymer in the series D experiments, with the catalyst samples in which titania is present only as anatase (S1, S4 and S5). Although the final amount of polymer formed was determined by weighting the reaction vial after the reaction mixture having been evaporated to constant weight, the polymer kinetic curves were calculated by difference, by assuming constant total mole number. The final amount obtained by weighting and the final polymer concentration obtained from the kinetic curves, were found to be in good agreement.

The coincidence between the abscissa time corresponding to the maximum of the limonene oxide profile and that corresponding to the inflexion point of the polymer profile, which seems to be observed in all cases, suggests that the polymer is formed from the epoxide, also being in agreement with previous observations [34]. Polymerisation is probably initiated on acid sites, proceeding via a cationic mechanism.

On the other hand, for the series D experiments carried out with the catalyst samples containing both titania polymorfs, anatase and rutile (S2 and S3—Fig. 4), such coincidence in time abscissas is not observed and no relation can be found between limonene oxide and the polymer. In both cases the polymer seems to be formed directly from limonene, after a long induction period. Polymerisation is likely to take place via a free radical chain reaction mechanism, the long induction period corresponding to the time needed for the propagation of free radicals generated on the vanadium sites, to the homogeneous phase.

The formation of limonene glycol in both C and D series is also an indication of the acidic activity exhibited by the catalyst

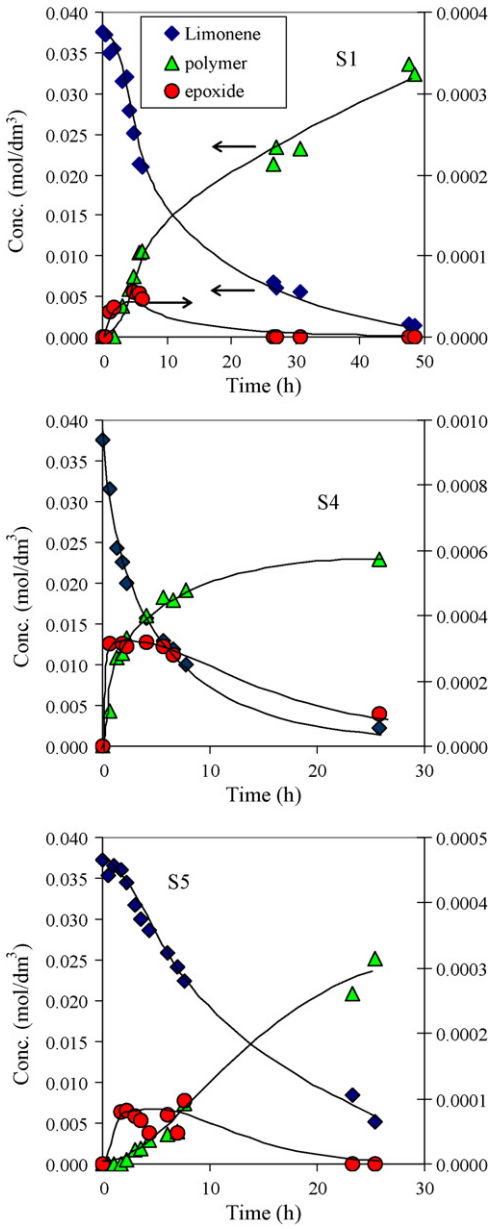

Fig. 3. Liquid phase limonene oxidation over V_2O_5/TiO_2 catalysts, using diluted (series D) *t*-BHP as oxygen donor. Concentration profiles of limonene, limonene oxide and polymer obtained with the anatase catalysts.

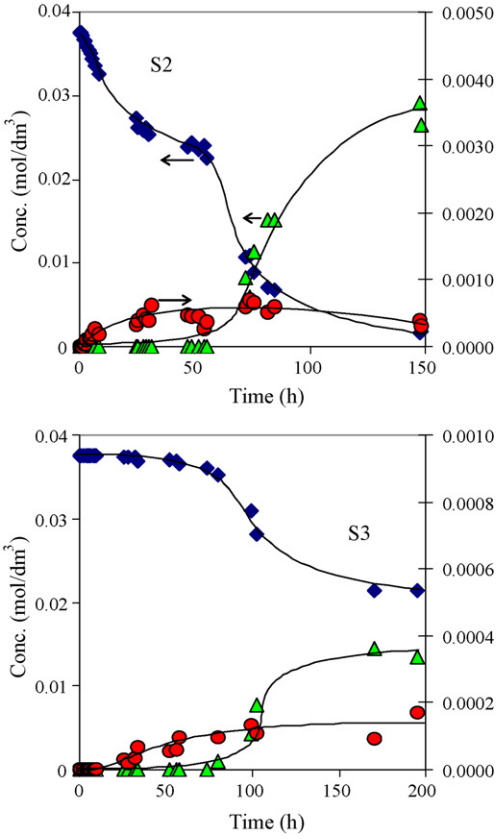

Fig. 4. Liquid phase limonene oxidation over V_2O_5/TiO_2 catalysts, using diluted (series D) *t*-BHP as oxygen donor. Concentration profiles of limonene, limonene oxide and polymer obtained with the anatase + rutile catalysts.

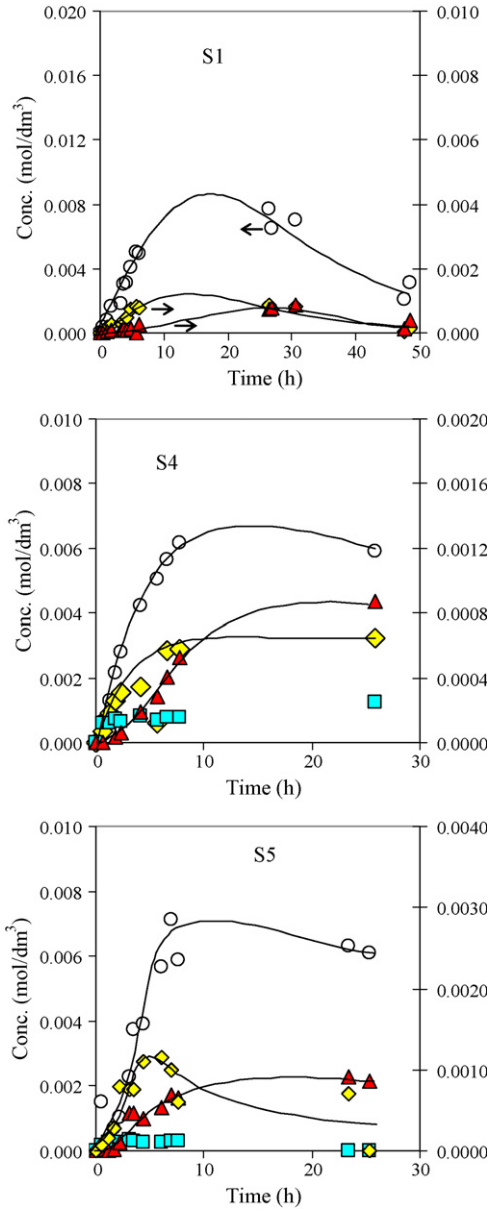

Fig. 5. Liquid phase limonene oxidation over V_2O_5/TiO_2 catalysts, using diluted (series D) *t*-BHP as oxygen donor. Concentration profiles of limonene glycol, carveol, carvone and "others" obtained with the anatase catalysts.

samples, since limonene glycol is likely to be formed by acid catalysed hydration of limonene oxide. In the experiments carried out with the anatase samples S1, S4 and S5, the time abscissas of the maximum values of the glycol concentration profiles seem to fit those of the inflexion points of carvone concentration profiles (Fig. 5). These observations suggest that these catalyst samples bear acid sites strong enough to promote the fast dehydration of limonene glycol to carveol, which is then readily oxidised to carvone.

For the experiments carried out with the anatase + rutile samples, S2 and S3, the above fittings of time abscissas are not observed (Fig. 6). Therefore, carveol seems not to be formed from limonene glycol. It is likely to be formed via limonene autoxidation instead.

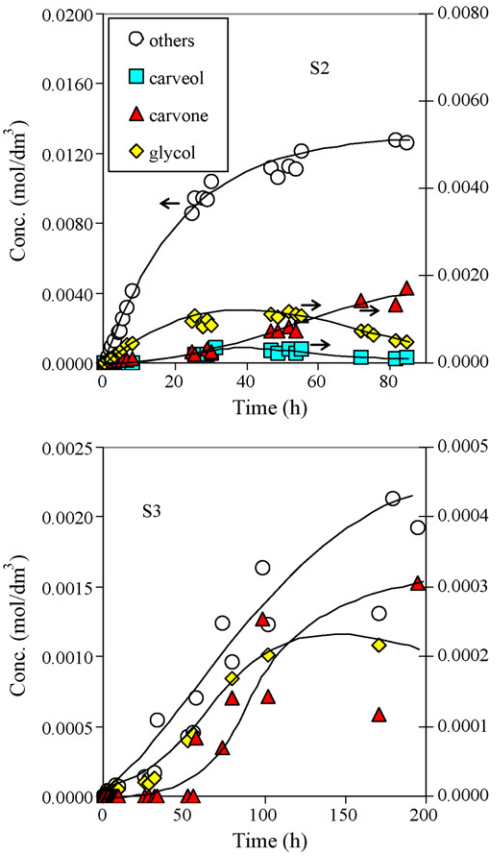

Fig. 6. Liquid phase limonene oxidation over V_2O_5/TiO_2 catalysts, using diluted (series D) *t*-BHP as oxygen donor. Concentration profiles of limonene glycol, carveol, carvone and "others" obtained with the anatase + rutile catalysts.

4. Conclusions

Two different groups of V_2O_5/TiO_2 were obtained: samples S1, S4, S5 and S6 contain titania only as anatase, while samples S2 and S3 exhibit both polymorphs, anatase and rutile.

All the catalyst samples seem to be active in limonene oxidation. However, when diluted *t*-BHP is used as oxidant, only the samples bearing vanadia on the particles outer surface (all but S6) are active. This means that limonene oxidation takes only place on the vanadium sites.

With the anatase samples (S1, S4 and S5) limonene oxide seems to be a primary reaction product. Apparently, polymerisation takes place from this product. Carveol and carvone seem to be formed also from limonene oxide, via limonene glycol: this compound would be formed by the acid catalysed epoxide hydration; then carveol may be formed from limonene glycol also through acid catalysed dehydration; finally carveol may be oxidised to carvone.

With the anatase + rutile samples (S2 and S3) a polymer is only formed after a long induction period, apparently directly from limonene. Although limonene oxide and limonene glycol are also found as reaction products, carveol and carvone seem to be also formed directly from limonene, by allylic oxidation. With these catalysts limonene autoxidation seems to be favoured.

Acknowledgements

This work was carried out with support from the POCTI-FEDER Programme (Project POCTI/CTM/45449/2002). P. Oliveira acknowledges the grant received under the same programme.

References

[1] M.J. Silva, P. Robles-Dutenhefner, L. Menini, E.V. Gusevskaya, J. Mol. Catal. A: Chem. 201 (2003) 71.
[2] N.K.K. Raj, V.G. Puranik, C. Gopinathan, A.V. Ramaswamy, Appl. Catal. A: Gen. 256 (2003) 265.
[3] M.V. Cagnoli, S.G. Casuscelli, A.M. Alvarez, J.F. Bengoa, N.G. Gallegos, N.M. Samaniego, M.E. Crivello, G.E. Ghione, C.F. Pérez, E.R. Herrero, S.G. Marchetti, Appl. Catal. A: Gen. 287 (2005) 227.
[4] B.M. Weckhuysen, D.E. Keller, Catal. Today 78 (2003) 25.
[5] G.C. Bond, Appl. Catal. A: Gen. 157 (1997) 91.
[6] K. Inumaru, M. Misono, T. Okuhara, Appl. Catal. A: Gen. 149 (1997) 133.
[7] B. Grzybowska-Swierkoz, Appl. Catal. A: Gen. 157 (1997) 263.
[8] I.E. Wachs, B.M. Weckhuysen, Appl. Catal. A: Gen. 157 (1997) 67.
[9] C.B. Rodella, P.A.P. Nascente, R.W.A. Franco, C.J. Magon, V.R. Mastelaro, A.O. Florentino, Phys. Stat. Sol. 187 (2001) 161.
[10] M. Khader, J. Mol. Catal. A: Gen. 105 (1995) 87.
[11] R.G. Dosch, H.P. Stephen, F.V. Stohl, US Patent 4,511,455 (1985).
[12] D.A. Chang, Y.H. Choh, W.F. Hsieh, P. Lin, T.Y. Tseng, J. Mater. Sci. 28 (1993) 6691.
[13] A. Ueno, H. Suzuki, Y. Kotera, J. Chem. Soc., Faraday Trans. 79 (1983) 127.
[14] F. Chiker, J.Ph. Nogier, J.L. Bonardet, Catal. Today 78 (2003) 139.
[15] D. Robba, D.M. Ori, P. Sangalli, G. Chiarello, L.E. Depero, F. Parmigiani, Surf. Sci. 380 (1997) 311.
[16] G.S. Wong, M.R. Concepcion, J.M. Vohs, Surf. Sci. 56 (2003) 211.
[17] J. Brinker, G. Scherer, Sol–Gel Science, Academic Press, New York, 1989 .
[18] L.G. Hubert-Pfalzgraf, New J. Chem. 11 (1987) 663.
[19] M.L. Rojas-Cervantes, R.M. Martín-Aranda, A.J. López-Peinado, J. de D. López-González, J. Mater. Sci. 29 (1994) 3743.
[20] B.E. Yoldas, J. Mater. Sci. 21 (1986) 1087.
[21] T. López, A. Hernández, X. Bokhimi, L. Torres-Martinez, A. García, G. Pecchi, J. Mater. Sci. 39 (2004) 565.
[22] A. Bokhimi, A. Morales, O. Novaro, T. López, E. Sánchez, R. Gómez, J. Mater. Res. 10 (1995) 2788.
[23] S.I. Niwa, F. Mizukami, S. Isoyama, T. Tsuchiya, K. Shimizu, S. Imai, J. Imamura, J. Chem. Technol. Biotechnol. 36 (1986) 236.
[24] F.C. Gennari, D.M. Pasquevich, J. Mater. Sci. 33 (1998) 1571.
[25] P. Scherrer, Estimation of the Size and Internal Structure of Colloidal Particles by Means of Roentgen Rays, Nachr. Ges. Wiss., Gottingen, 1918 p. 96.
[26] K. Tenabe, K. Kato, H. Miyazaki, S. Yamaguchi, A. Imai, Y. Iguchi, J. Mater. Sci. 29 (1994) 1617.
[27] E.F. Heald, C.W. Weiss, Am. Mineral. 57 (1972) 10.
[28] M. Ocaña, J.V. Garcia-Ramos, C.J. Serna, J. Am. Ceram. Soc. 75 (1992) 201.
[29] A. Mills, R.H. Davies, D. Worsley, Chem. Soc. Rev. (1993) 417.
[30] C.M. Casttilla, A.P. Cadenas, F.M. Hódar, F.C. Marín, J.L. Fierro, Carbon 41 (2003) 1157.
[31] L.K. Boudali, A. Ghorbel, P. Grange, F. Figueras, Appl. Catal. B: Environ. 59 (2005) 105.
[32] G.S. Wong, M.R. Conception, J.M. Vohs, Surf. Sci. 526 (2003) 211.
[33] M.L. Rojas-Cervantes, A.J. Lopez-Peinado, J. de D. Lopez-González, F. Carrasco-Marín, J. Mater. Sci. 31 (1996) 437.
[34] P. Oliveira, A.M. Ramos, I. Fonseca, A.M.B. do Rego, J. Vital, Catal. Today 102–103 (2005) 67.